Article:
Xu, F, Wu, X, Jiang, L-H et al. (2016) An organelle K^+ channel is required for osmoregulation in Chlamydomonas reinhardtii. Journal of Cell Science, 129 (15). pp. 3008-3014. ISSN: 0021-9533

https://doi.org/10.1242/jcs.188441

An organelle K^+ channel is required for osmoregulation in *Chlamydomonas reinhardtii*

Feifei Xu[a], Xiaoan Wu[b], Lin-Hua Jiang[c], Hucheng Zhao[b,1] and Junmin Pan[a,d,1]

[a]MOE Key Laboratory of Protein Sciences, School of Life Sciences, Tsinghua University, Beijing, China

[b]Lab of Biomechanics, Department of Engineering Mechanics, Tsinghua University, Beijing, China

[c]School of Biomedical Sciences, University of Leeds, Leeds LS2 9JT, U.K.

[d]Laboratory for Marine Biology and Biotechnology, Qingdao National Laboratory for Marine Science and Technology, Qingdao, Shandong Province, China

Running title: Osmoregulation by a CV potassium channel

[1]Correspondence:

panjunmin@tsinghua.edu.cn; Tel/Fax 0086-1062771864

zhaohc@mail.tsinghua.edu.cn; Tel/Fax 0086-1062782771

Fresh water protozoa and algae face hypotonic challenges in their living environment. Many of them employ a contractile vacuole (CV) system to uptake excessive water from the cytoplasm and expel it to the environment to achieve cellular homeostasis. Potassium, a major osmolyte in CV, is predicted to create higher osmolarity for water influx. Molecular mechanisms for K^+ permeation through plasma membrane have been well studied. How K^+ permeates organelles such as CV is not clear. Here, we show that a six-transmembrane K^+ channel KCN11 in *Chlamydomonas* is exclusively localized to CV. Ectopic expression of KCN11 in HEK293T cells results in voltage-gated K^+ channel activity. Disruption of the gene or mutation of key residues for K^+ permeability of the channel leads to dysfunction of cell osmoregulation in very hypotonic conditions. The contractile cycle is inhibited in the mutant cells with slower rate of CV swelling, leading to cell death. These data demonstrate a new role for six transmembrane potassium channels in the CV functioning and provide further insights into osmoregulation mediated by contractile vacuole.

Key words: *Chlamydomonas;* Contractile vacuole; Osmoregulation; Potassium channel

Fresh water living organisms such as protozoa and algae are subjected to a hypotonic condition. The osmolality of fresh water is typically below 7 mOsm, whereas the cytosolic osmolality of fresh water protozoa is estimated to be 45 - 117 mOsm (Allen and Naitoh, 2002). In *Chlamydomonas reinhardtii*, it was measured as 170 mOsm (Komsic-Buchmann et al., 2014). The osmotic pressure will allow water influx into the cytoplasm. Many of these cells utilize the contractile vacuole (CV) complex to expel excessive water out of the cell. Although the morphologies of CV complex vary among different protists, it generally consists of a central vacuole surrounded by numerous tubules and vesicles. At the initial stage of CV formation, small vesicles fuse to form a central vacuole, which gradually enlarges by continuous fusion of vesicles and active influx of water. Eventually the enlarged vacuole tethers with the plasma membrane and discharges water out of the cell. This process occurs periodically and is critical for cell growth and survival (Allen and Naitoh, 2002; Docampo et al., 2013).

The mechanism by which the CV extracts water from the cytoplasm is not well understood. Osmotic gradient built between the cytosol and CV has been proposed as the driving force for water uptake in the CV (Allen and Naitoh, 2002; Docampo et al., 2013; Riddick, 1968; Zeuthen, 1992).The osmolytes in the CV attract water that enters through the aquaporin water channels present on the CV membrane (Docampo et al., 2013; Komsic-Buchmann et al., 2014). While the compositions of the osmolytes in the CV fluid are disputed (Allen and Naitoh, 2002; Docampo et al., 2013), several studies suggest that K^+ is one of the major osmolytes. In an earlier report, Na^+ and K^+ were thought to account for most osmotically active cations of the vacuole in *Chaos carolinensis* (Riddick, 1968). Recently, direct measurement of the ion contents in the CV of *Paramecium multimicronucleatum* in vivo has demonstrated that K^+ and Cl^- serve as the major osmolytes (Stock et al., 2002). However, how K^+ enters the CV is not clear. Analysis of the CV membrane of *Dictyostelium discoideum* discovered the presence of voltage-dependent K^+ channel activity twenty years ago, however, the molecular identity of the channel has not been identified so far (Yoshida et al., 1997).

C. reinhardtii is a fresh water unicellular green alga. Two contractile vacuoles, which pulsate alternately, are present in the cell anterior, on opposite sides of the plane that include the flagellar basal bodies (Komsic-Buchmann et al., 2012; Luyk et al., 1997). In this work, we have identified a voltage-gated K^+ channel that is localized to the CV membrane of *C. reinhardtii,* and critically required for the CV cycling in water and functions in osmoregulation.

Results

K^+ channels in the *C. reinhardtii* genome

K^+ channels are conventionally classified into three structural classes based on the predicted membrane topology: the six transmembrane (TM) domain class (6TMs) with one K^+ selective pore domain, the four TM domain class (4TMs) with two pore domains and the two TM class (2TMs) with one pore domain (Huang and Jan, 2014). The consensus motif TXXTXGXGD with invariant Gs in the pore domain confers K^+ selective permeation (Doyle et al., 1998; Heginbotham et al., 1994; Yellen et al., 1991). In the *C. reinhardtii* genome database Phytozome v10.3, a total of 12 potassium channels have been annotated, including KCN1-9, KCA1, and IRK1-2. However, KCN5, 7, 8 and IRK2 are unlikely K^+ selective channels because no GXG triads are present in their putative pore domains.

To search for additional K^+ selective channels, protein sequences of the representative K^+ channels from higher plant *Arabidopsis thalina* and human were blasted in the *C. reindardtii* genome database. A total of 14 putative K^+ channels were identified with the new ones named KCN10-15 thereafter, respectively (Table S1, Fig. 1*A*). The putative K^+ channels are predicted to have 6TMs with IRK1 as an exception, which has 2TMs (Table S2). These data indicate that *C. reinhardtii* does not have the 4TM K^+ channels, which are present in human and higher plants (Hedrich, 2012; Moulton et al., 2003). The fourth segments (S4) of all the 6TM putative K^+ channels possess highly positively charged amino acids (Fig. 1*A*), indicating they can be gated

by a change in membrane potential (Jan and Jan, 1997). Phylogenetic analysis with representative members from *Arabidopsis* and human classified these channels into several distinctive groups including plant 6TMs, EAG, Kv, and Kir groups while some channels are not closely related to members of plant or human K^+ channels (Fig. 1*B*).

KCN11 encodes a bona fide K^+ channel and is mutated in a _C. reinhardtii_ strain

To analyze genes disrupted in *C. reinhardtii* insertional mutants which were generated by transforming a DNA fragment harboring paromomycin resistant gene *AphVIII* (Meng et al., 2014; Sizova et al., 2001), we found that *KCN11* was disrupted in one of the mutants by the insertion of this DNA fragment in the sixth exon of the gene (Fig. 2*A*). The genomic junction site of the insert at the 3' end is at 1810 nt. The sequence of the genomic junction site at the 5' end of the insert was unable to be defined. Further experiments with PCR showed that the 5' end of the insert is positioned between 1709 – 1809 nt, indicating that this insert disrupts the *KCN11* gene alone (Fig. S1). KCN11 encodes a protein of 800 amino acids. The predicted domain structure and membrane topology of KCN11 are depicted in Fig. 2*B*. The DNA insertion disrupted *KCN11* expression as examined by real-time RT-PCR, indicating that this insertion results in a null mutant (Fig. 2*C*). To determine whether *KCN11* encodes a K^+ channel, the cDNA of *KCN11* was expressed in HEK293T cells and whole-cell K^+ currents were measured using patch-clamp technique (Fig. 2*D*, *E*). Untransfected cells exhibited very small background leak current density (25.86±1.41 pA/pF at +60 mV, n=6). Cells expressing *KCN11* showed voltage-gated large outwardly rectifying K^+ currents (161.66±7.21 pA/pF at +60 mV, n=8), and treatment with the K^+ channel inhibitor TEA inhibited these currents to levels similar to those of the untransfected cells (27.61±3.96 pA/pF at +60 mV, n=7) (Fig. 2*E*). In contrast, treatment with nifedipine, a voltage-gated calcium channel blocker, or with tetrodotoxin, a voltage-gated sodium channel blocker, did not significantly inhibit K^+ currents (Fig. 2*D, E*). The peak K^+ current densities in *KCN11* transfected cells were measured in the presence of different concentrations of extracellular potassium ($[K]_o$) (Fig. 2*F*), and the relationship of the current reversal potential (E_{rev}) to $[K]_o$ was well fit to E_{rev}

=62*log*([K]$_o$/140) (Fig. 2*G*). These results provide clear evidence to show that KCN11 is K^+ selective. Thus, KCN11 functions as a voltage-gated K^+ selective channel with strong outward rectification.

KCN11 is localized to the membrane of CV

An HA-tagged *KCN11* was transformed into the *kcn11* mutant, which restored the expression of KCN11 (Fig. 2*C*). To determine the cellular localization of KCN11, positive transformants were analyzed by structured illumination microscopy (SIM) by using an anti-HA antibody with anti-α-tubulin antibody as control (Fig. 3*A*). Instead of localization to the plasma membrane, KCN11 was exclusively found at two vesicle-like structures located on each side of the base of the flagella, which are reminiscent of the two CVs (Komsic-Buchmann et al., 2012; Luyk et al., 1997). Three dimensional reconstructions of the images show that KCN11-HA staining exhibits two bladder like structures, indicating these structures are CVs (Fig. 3*B*).

KCN11 controls CV cycle and functions in osmoregulation

The *kcn11* mutant grew normally in normal growth condition (see Materials and Methods), and no apparent phenotypes including cell motility and cellular structures were observed. As KCN11 was localized to the CV membrane, we examined the CV functional properties of the cells. In the growth medium, the average CV periods between wild type (WT) cells and *kcn11* mutants were similar, with 20.72±0.53 sec (n=45) for WT cells and 20.43±0.51 sec (n=45) for the mutants, which are consistent with previous report (Komsic-Buchmann et al., 2012) (Fig. 4*A* and *B*). Neither did we observe significant differences in the CV size (Fig. 4*C*). These data indicate that KCN11 is not critically involved in osmoregulation in the growth medium.

Next, we examined the CV cycles of the cells in water, a very hypotonic condition. The CV diameters did not change (Fig. 4*C*). Interestingly, *KCN11* expression was increased when cells were grown under such hypotonic condition (Fig. S2). Consistent with the previous report (Luyk et al., 1997), WT cells exhibited a rapid CV

cycling. WT cells had a shortened CV period of 10.98±0.37 sec (n=45), with 47% increase in the CV cycling rate. In contrast, the *kcn11* cells showed a CV period of 15.53±0.44 sec (n=45), with only 23% increase in the CV cycling rate (Fig. 4*B*). Thus, *kcn11* cells exhibited around 50% reduction in the CV cycling rate compared to WT cells. The rescued strain restored the defect in CV contraction of the mutant (Fig. 4B). Taken together, these results suggest that *KCN11* gene expression is important in the regulation of the CV activity. The CV systoles of WT and *kcn11* cells were similar, with 0.91±0.04 sec (n=30) for WT cells and 1.02±0.05 sec (n=30) for *kcn11* cells. Thus, KCN11 plays a critical and exclusive role in the diastole, i.e. the water accumulation stage. To further elaborate whether the K^+ channel activity of KCN11 is required for the CV activity, a triple mutant (T392G/V394E/G395E) in the K^+ selective filter (filter mutant) was generated, which is predicted to abolish the K^+ channel activity (Heginbotham et al., 1994). As expected, whole-cell recording showed that the filter mutant was defective in K^+ conductance (Fig. 2*D* and *E*). The filter mutant was transformed into *kcn11* cells and similarly expressed as the transformed WT gene in *kcn11* cells (Fig. S3). However, unlike the WT *KCN11*, the filter mutant failed to rescue the CV phenotype of the *kcn11* mutant (Fig. 4*B*), indicating that KCN11 channel function is required for regulating the CV activity.

The defects in CV activity related osmoregulation should affect cell growth and survival. Cells were grown on agar plates prepared with water. The cells from WT and rescued strains grew apparently normally in the test period of three days (Fig. 4*D*). In contrast, *kcn11* null and filter mutants did not grow and appeared dying. The cells were then grown in water for examination of cell viability (Fig. 4*E* and *F*). As expected, within 3 days, almost all cells from *kcn11* null and filter mutants were dead whereas WT and rescued cells were still viable. These data suggest that KCN11-depedent CV activity is crucial for cell growth and survival under very hypotonic condition.

Discussion

We have discovered a 6TM K^+ channel KCN11 that is located in the CV membrane of

C. reinhardtii. KCN11 shows voltage-gated outwardly rectifying activity and supposedly mediates K^+ permeation into the CV. Indeed, null mutants or mutants defective in selective K^+ permeation activity exhibit an increase of the CV periods and lose their capacity to mediate osmoregulation under very hypotonic condition leading to cell death. To our knowledge, this is the first study reporting the identity and function of a K^+ channel in the CV membrane of any protists.

During diastole of the CV cycle, liquid-filled vesicles continue to fuse with the CV (Allen and Naitoh, 2002; Komsic-Buchmann et al., 2012; Luyk et al., 1997; Parkinson et al., 2014). Vesicle fusion requires the function of exocyst as CV formation is compromised in a *sec6* mutant in *C. reinhardii* (Komsic-Buchmann et al., 2012). In *D. discoideum*, an ATP-sensitive P2X receptor ion channel that is localized to the CV regulates organellar calcium homeostasis and vesicle fusion during CV formation (Fountain et al., 2007; Parkinson et al., 2014). However, vesicle fusion alone should result in flaccid vacuole. Additional transport of water into CV driven by osmosis should be required. The osmolytes that account for the osmolarity in the CV has been disputed. Bicarbonate and ammonium have been proposed to serve as major osmolytes though no direct evidence has been shown (Docampo et al., 2013; Heuser et al., 1993). In *Trypanosome cruzi*, it has also been postulated that hydrolysis of polyphosphate after the fusion of acidocalcisomes with the CV complex may result in an increase in phosphates and cations, leading to an increase of the osmolarity of the CV (Rohloff and Docampo, 2008). Analysis of *in vivo* CV ion contents in *P. multimicronucleatum* has identified K^+ as one of the major osmolytes (Stock et al., 2002). The present study showed that KCN11 expression is increased under a very hypotonic condition and KCN11 is located in the CV membrane. Furthermore, the cells harboring null or non-functional *KCN11* mutants have reduced CV activities with prolonged diastole and could not survive in a very hypotonic condition. Such functional defects were well rescued by re-introduction of wild-type *KCN11* expression. These results provide compelling evidence to support a critical role of the KCN11 K^+ channel in the osmoregulation under a very hypotonic condition. How the KCN11

channel activity is regulated is currently unknown. It has a nucleotide binding domain, indicating that it is likely regulated by cAMP or cGMP. However, the K^+ channel activity detected in the CV membrane of *D. discoideum* was not affected by these nucleotides (Yoshida et al., 1997). Further studies are needed to learn more about the regulation of the expression and activity of KCN11 K^+ channels present in the CV membrane.

kcn11 mutants were defective in osmoregulation in water and could not survive. However, in culture medium which has a higher osmolarity, *kcn11* mutants grew normally and their CV activity was not affected. The underlying mechanism is currently unknown. Other K^+ channel or transporters may be involved or cells may use different osmolytes to control the CV cycle and osmolarity.

Compared to the K^+ channels in the plasma membranes, the molecular identities and functions of K^+ channels in the intracellular membranes have not been well studied. Recently, in mammalian cells, a novel K^+ channel with two repeats of 6TM domains has been localized in the membranes of lysosomes and endosomes and mediates organelle K^+ release to regulate lysosomal function (Cang et al., 2015). In higher plants, the vacuole plays a similar functional role as CV in osmoregulation (Becker, 2007). Four 4TM K^+ channels including TPK1, 2, 3 and 5 are located in the vacuole membranes (Voelker et al., 2006). TPK1 regulates vacuolar K^+ release and functions in stomatal closure (Czempinski et al., 2002; Gobert et al., 2007). Though *C. reinhardtii* shares a common ancestor with higher plants, no 4TM K^+ channels have been found in our analysis. Thus, the organelle K^+ channel KCN11 is novel in that it is a 6TM channel and regulates K^+ entry into an organelle and plays an important role in osmoregulation.

Materials and Methods

Strains, culture conditions and cell tranfection

C. reinhardtii strain *21gr* (mt+) (CC-1690) is available from the *Chlamydomonas* Genetics Center, University of Minnesota. Cells were cultured in 250 ml Erlenmeyer flasks at 23˚C with aeration under 14:10 hour light-dark cycle. The culture medium used is M medium (Minimal medium or Medium I) (Sager and Granick, 1954). The osmolarity of the medium is 20 mOsm, which was determined using a freezing point depression osmometer (OM806, Loeser Messtechnik, Berlin, Germany). For cells growing in water, cells were simply grown in distilled water or water-prepared 1.5% agar plates under continuous light. For mammalian cell transfection, human embryonic kidney 293T (HEK293T) cells (ATCC) were maintained in 6-well plates in DMEM with 10% FBS and transfected with Lipofectamine 2000 (Invitrogen).

Bioinformatic analysis

To identify additional K^+channels and verify the annotated channels, we have searched the *C. reinhardtii* proteome (Phytozome 10.3) by Blast followed by determination of the presence of K^+ channel signature motif GXG. To ensure recovery of all the K^+ channels, the protein sequences from representative members of 6TM, 4TM and 2TM K^+ channels of higher plant *A. thalina* and human were used for Blast. The protein sequences used are: S5-S6 segment of 6TM K^+ channel SKOR (Q9M8S6), S1-S4 segment of 4TM TPK1 (Q8LBL1) and S1-S2 segment of 2TM KCO3 (Q9XFR0) of *A. thalina*; S5-S6 segment of 6TM KCNH1 (O95259), S1-S4 segment of 4TM KCNK1 (O00180) and S1-S2 segment of 2TM KCNJ1 (P48048) of human. The transmembrane regions of the putative channels were predicted by using SMART (http://smart.embl-heidelberg.de), Hmmtop (http://www.enzim.hu/hmmtop) and TMHMM (http://www.cbs.dtu.dk/services/TMHMM-2.0/). Other domains were predicted by SMART.

A neighbor-Joining tree was built by using the software Mega 6 (Tamura et al., 2013).

The proteins analyzed include the following: 14 putative K^+ channels of *C. reinhardtii* (for accession numbers, see Table S1), 6 representative members from *A. thalina* (Hedrich, 2012) (SKOR (Q9M8S6), AKT2/3 (Q38898), KAT3 (P92960), KAT1 (Q39128), TPK1 (Q8LBL1), KCO3 (Q9XFR0)) and 7 representative members from human (Moulton et al., 2003) (KCMA1 (Q12791), KCNN1 (Q92952), KCNA1 (Q09470), KCNQ1 (P51787), KCNH1 (O95259), KCNJ1 (P48048), KCNK1 (O00180)). The transmembrane domains were used for analysis.

Insertional mutagenesis, gene cloning, and other molecular techniques

Insertional mutants were generated by transformation of *C. reinhardtii* with electroporation of *AphVIII* fragments (Liang and Pan, 2013; Sizova et al., 2001). Flanking sequence of the DNA insert was identified by RESDA PCR and sequencing (Gonzalez-Ballester et al., 2005; Meng et al., 2014). To make a construct for rescuing *kcn11*, *KCN11* gene with an approximately 2 kb fragment upstream of the start codon was cloned by PCR using Phanta Max Super-Fidelity DNA Polymerase (Vazyme Biotech Co. Ltd, Nanjing, China) from a bac clone BAC31O7 (Clemson University, USA) and a 3×HA tag sequence followed by a LC8 terminator was cloned from plasmid pKL-3xHA (kindly provided by Karl F. Lechtreck, University of Georgia) (Lechtreck et al., 2009). The resulting DNA fragment was cloned into a modified vector pHyg3 harboring a hygromycine B resistance gene (Berthold et al., 2002). The final construct pHyg3-KCN11-HAwas linearized with ScaI-HF and transformed into*kcn11* mutant.To make the K^+ selection filter mutant, the DNA sequence encoding TMTTVGYGD (5'- ACCATGACCACCGTGGGGTACGGAGAC-3') was replaced with the DNA sequence (5'- ACCATGGGCACCGAGGAGTACGGAGAC-3') that encodes TMGTEEYGD.

To express *KCN11* in mammalian cells, a cDNA was cloned by PCR from a cDNA library of *C. reinharditi* with NheI and BamHI restriction sites added at the 5' and 3' ends, respectively. This DNA fragment was cloned into pIRES2-EGFP (kindly provided by Dr. Xiaodong Liu, Tsinghua University).

Total RNA was extracted using Trizol (Invitrogen), and reverse transcribed into cDNA using PrimeScript® RT reagent Kit (Takara, Japan). RNA quantification was performed using SYBR Green Premix Ex Taq (Takara, Japan) on Thermal Cycler Dice Real Time System II. CBLP was used as control. Primers used are: *KCN11*, 5'-AGCTGTTCGTGGTGCTGTACA-3' and 5'-CGCGAATGACGTAGTCGCTT-3'; *CBLP*, 5'-ATGTGCTGTCCGTGGCTTTC-3' and 5'-GCCCACCAGGTTGTTCTTCA-3'.

Patch-clamp current recordings

The recording chamber was perfused with extracellular solution (0.5ml/min) containing the following (in mM): 135 NaCl, 5 KCl, 2 $CaCl_2$, 1 $MgCl_2$, 5 HEPES, 10 glucose, pH 7.4 with NaOH, 310 mOsm. The pipette solution contained the following (in mM): 140 KCl, 1 EGTA, 2 $MgCl_2$, 1 ATP-Mg, 0.1 GTP-Na, 5 HEPES, 10 Tris-phosphocreatine, 10 units/ml creatine phosphokinase, pH 7.3 with KOH, 290 mOsm. For the blocker experiments, extracellular solutions contained 1 mM Tetraethylammonium chloride (TEA), 10 mM nifedipine, or 1 mM Tetrodotoxin (TTX) were used to examine their effects on the K^+ currents. Recording pipettes had around 3.5 MΩ resistance. Series resistance (15 MΩ, average 8.9± 0.2 MΩ) was compensated by 70%. Current traces were corrected with online P/6 trace subtraction using scaled hyperpolarizing steps. Signals were filtered at 2 kHz and digitized at 10 kHz. To measure the current–voltage relationships (I–V curves) of K^+ channels, the membrane potential was held at -60 mV. Command steps from -100 mV to +60 mV (10 mV increments) were applied for 500 ms. For each cell, the peak current was normalized by the membrane capacitance (a measure of cell surface area) to obtain current density (Liu et al., 2013). The reversal potentials (E_{rev}) were derived from the current density-membrane potential relationship curves in the extracellular solutions containing different K+ concentrations ($[K^+]_o$) (5, 20, 100, and 140 mM KCl), while the intracellular K^+ concentration was kept at 140 mM. For assay of transfected cells, one day after transfection, the cells were seeded on Matrigel-coated coverslips. Transfected cells were identified by the EGFP fluorescence and used for patch-clamp

recordings 2–3 d after transfection. The data are presented in mean ± SEM.

SDS-PAGE and immunoblotting

SDS-PAGE and immunoblotting analysis were essentially as described previously (Cao et al., 2013). Primary antibodies used are rat monoclonal anti-HA (1:2,000, clone 3F10, Roche), mouse monoclonal anti-α-tubulin (1:10,000, Sigma) and rabbit anti-CrCDPK3 antibody (Liang and Pan, 2013; Sizova et al., 2001).

Immunofluorescence microscopy

Immunofluorescence imaging was carried out as detailed in a previous study (Hu et al., 2015). The primary antibodies and the secondary antibodies used are as follows: mouse anti-α-tubulin (1:100, Sigma), rat anti-HA (1:50, Roche), Texas Red goat anti-mouse IgG (1:200) and Alexa Fluor 488 goat anti-rat IgG (1:200) (Invitrogen). The samples were viewed on anN-SIM microscope (Nikon) equipped with an Andor EMCCD camera (897, Andor) using 100x objective (NA1.49). The images were acquired and processed by NIS-Element4.4 (Nikon) and Adobe softwares (Adobe). Imaris software (Bitplane) was used for three-dimensional reconstruction.

Live cell imaging

The cell viability assay was performed following a previously published protocol (Yordanova et al., 2010). In brief, a stock fluorescein diacetate (FDA) (Sigma, Shanghai, China) solution was prepared in advance by dissolving 5 mg/ml in DMSO and stored at -20^{o}C. Cells grown in M medium were incubated in water for growing. At different times as indicated, cells were stained with FDA (20 μg/ml, final concentration) for five min in the dark at room temperature. The samples were captured under Zeiss Axio Observer Z1 microscope equipped with a CCD camera (QuantEM 512SC, Photometrics) using a 40x objective. Images were exported and processed using Photoshop and Illustrator (Adobe).

For imaging the CV cycle, two microscopy imaging systems were used. For statistical

analysis, the cells were imaged with the microscopy system described above. The images were taken every 50 ms, exported and processed using Adobe Photoshop and ImageJ (NIH) for analysis. The CV cycles and diameters were plotted (GraphPad Prism) and statistical analysis was preformed (Student's *t*-test). For imaging cells in water, cells were adapted in water for 1 hr before imaging. For the videos presented, cells were viewed on a Zeiss LSM780 META Observer Z1 Confocal Laser Microscope with 100x objective (NA1.40). Images were acquired and processed by ZEN 2009 Light Edition (Zeiss), Adobe softwares (Adobe) and ImageJ (NIH). The videos were generated using Windows Movie Maker (Microsoft).

ACKNOWLEDGMENTS

We thank Drs. Xiaodong Liu, Tsinghua University and Karl Lechtreck, University of Georgia for providing plasmids and Center of Biomedical Analysis, Tsinghua University for assistance with imaging analysis. This work was supported by National Natural Science Foundation of China (31172405 and 31330044) (to J. P.).

References

Allen, R. D. and Naitoh, Y. (2002). Osmoregulation and Contractile Vaccuoles of Protozoa. *Int. Rev. Cytol.* **215**, 351-394.

Becker, B. (2007). Function and evolution of the vacuolar compartment in green algae and land plants (Viridiplantae). *Int. Rev. Cytol.* **264**, 1-24.

Berthold, P., Schmitt, R. and Mages, W. (2002). An engineered Streptomyces hygroscopicus aph 7" gene mediates dominant resistance against hygromycin B in Chlamydomonas reinhardtii. *Protist* **153**, 401-412.

Cang, C., Aranda, K., Seo, Y. J., Gasnier, B. and Ren, D. (2015). TMEM175 Is an Organelle K(+) Channel Regulating Lysosomal Function. *Cell* **162**, 1101-1112.

Cao, M., Meng, D., Wang, L., Bei, S., Snell, W. J. and Pan, J. (2013). Activation loop phosphorylation of a protein kinase is a molecular marker of organelle size that dynamically reports flagellar length. *Proc. Natl. Acad. Sci. U S A* **110**, 12337-12342.

Czempinski, K., Frachisse, J. M., Maurel, C., Barbier-Brygoo, H. and Mueller-Roeber, B. (2002). Vacuolar membrane localization of the Arabidopsis 'two-pore' K+ channel KCO1. *Plant J.* **29**, 809-820.

Docampo, R., Jimenez, V., Lander, N., Li, Z. H. and Niyogi, S. (2013). New insights into roles of acidocalcisomes and contractile vacuole complex in osmoregulation in protists. *Int. Rev. Cell Mol. Biol.* **305**, 69-113.

Doyle, D. A., Morais Cabral, J., Pfuetzner, R. A., Kuo, A., Gulbis, J. M., Cohen, S. L., Chait, B. T. and MacKinnon, R. (1998). The structure of the potassium channel: molecular basis of K+ conduction and selectivity. *Science* **280**, 69-77.

Fountain, S. J., Parkinson, K., Young, M. T., Cao, L., Thompson, C. R. and North, R. A. (2007). An intracellular P2X receptor required for osmoregulation in Dictyostelium discoideum. *Nature* **448**, 200-203.

Gobert, A., Isayenkov, S., Voelker, C., Czempinski, K. and Maathuis, F. J. (2007). The two-pore channel TPK1 gene encodes the vacuolar K+ conductance and plays a role in K+ homeostasis. *Proc. Natl. Acad. Sci. U S A* **104**, 10726-10731.

Gonzalez-Ballester, D., de Montaigu, A., Galvan, A. and Fernandez, E. (2005). Restriction enzyme site-directed amplification PCR: a tool to identify regions flanking a marker DNA. *Anal. Biochem.* **340**, 330-335.

Hedrich, R. (2012). Ion channels in plants. *Physiol. Rev.* **92**, 1777-1811.

Heginbotham, L., Lu, Z., Abramson, T. and MacKinnon, R. (1994). Mutations in the K+ channel signature sequence. *Biophys J.* **66**, 1061-1067.

Heuser, J., Zhu, Q. and Clarke, M. (1993). Proton pumps populate the contractile vacuoles of Dictyostelium amoebae. *J. Cell Biol.* **121**, 1311-1327.

Hu, Z., Liang, Y., He, W. and Pan, J. (2015). Cilia disassembly with two distinct phases of regulation. *Cell Rep.* **10**, 1803-1810.

Huang, X. and Jan, L. Y. (2014). Targeting potassium channels in cancer. *J Cell Biol* **206**, 151-162.

Jan, L. Y. and Jan, Y. N. (1997). Ways and means for left shifts in the MaxiK channel. *Proc. Natl. Acad. Sci. U S A* **94**, 13383-13385.

Komsic-Buchmann, K., Stephan, L. M. and Becker, B. (2012). The SEC6 protein is required for contractile vacuole function in Chlamydomonas reinhardtii. *J. Cell Sci.*

125, 2885-2895.
Komsic-Buchmann, K., Wostehoff, L. and Becker, B. (2014). The contractile vacuole as a key regulator of cellular water flow in Chlamydomonas reinhardtii. *Eukaryot. Cell* **13**, 1421-1430.
Lechtreck, K. F., Luro, S., Awata, J. and Witman, G. B. (2009). HA-tagging of putative flagellar proteins in Chlamydomonas reinhardtii identifies a novel protein of intraflagellar transport complex B. *Cell Motil. Cytoskeleton* **66**, 469-482.
Liang, Y. and Pan, J. (2013). Regulation of flagellar biogenesis by a calcium dependent protein kinase in Chlamydomonas reinhardtii. *PLoS One* **8**, e69902.
Liu, P., Xiao, Z., Ren, F., Guo, Z., Chen, Z., Zhao, H. and Cao, Y. Q. (2013). Functional analysis of a migraine-associated TRESK K+ channel mutation. *J. Neurosci.* **33**, 12810-12824.
Luyk, P., Hoppenrath, M. and Robinson, D. G. (1997). Structure and behavior of contractile vacuoles in Chlamydomonas reinhardtii. *Protoplasma* **198**, 73-84.
Meng, D., Cao, M., Oda, T. and Pan, J. (2014). The conserved ciliary protein Bug22 controls planar beating of Chlamydomonas flagella. *J. Cell Sci.* **127**, 281-287.
Moulton, G., Attwood, T. K., Parry-Smith, D. J. and Packer, J. C. (2003). Phylogenomic analysis and evolution of the potassium channel gene family. *Receptors Channels* **9**, 363-377.
Parkinson, K., Baines, A. E., Keller, T., Gruenheit, N., Bragg, L., North, R. A. and Thompson, C. R. (2014). Calcium-dependent regulation of Rab activation and vesicle fusion by an intracellular P2X ion channel. *Nat. Cell Biol.* **16**, 87-98.
Riddick, D. H. (1968). Contractile vacuole in the amoeba Pelomyxa carolinensis. *Am. J. Physiol.* **215**, 736-740.
Rohloff, P. and Docampo, R. (2008). A contractile vacuole complex is involved in osmoregulation in Trypanosoma cruzi. *Exp. Parasitol.* **118**, 17-24.
Sager, R. and Granick, S. (1954). Nutritional control of sexuality in Chlamydomonas reinhardi. *J. Gen. Physiol.* **37**, 729-742.
Sizova, I., Fuhrmann, M. and Hegemann, P. (2001). A Streptomyces rimosus aphVIII gene coding for a new type phosphotransferase provides stable antibiotic resistance to Chlamydomonas reinhardtii. *Gene* **277**, 221-229.
Stock, C., Gronlien, H. K., Allen, R. D. and Naitoh, Y. (2002). Osmoregulation in Paramecium: in situ ion gradients permit water to cascade through the cytosol to the contractile vacuole. *J. Cell Sci.* **115**, 2339-2348.
Tamura, K., Stecher, G., Peterson, D., Filipski, A. and Kumar, S. (2013). MEGA6: Molecular Evolutionary Genetics Analysis version 6.0. *Mol. Biol. Evol.* **30**, 2725-2729.
Voelker, C., Schmidt, D., Mueller-Roeber, B. and Czempinski, K. (2006). Members of the Arabidopsis AtTPK/KCO family form homomeric vacuolar channels in planta. *Plant J.* **48**, 296-306.
Yellen, G., Jurman, M. E., Abramson, T. and MacKinnon, R. (1991). Mutations affecting internal TEA blockade identify the probable pore-forming region of a K+ channel. *Science* **251**, 939-942.
Yordanova, Z. P., Iakimova, E. T., Cristescu, S. M., Harren, F. J., Kapchina-Toteva, V. M. and Woltering, E. J. (2010). Involvement of ethylene and nitric oxide in cell

death in mastoparan-treated unicellular alga Chlamydomonas reinhardtii. *Cell Biol. Int.* **34**, 301-308.

Yoshida, K., Ide, T., Inouye, K., Mizuno, K., Taguchi, T. and Kasai, M. (1997). A voltage- and K+-dependent K+ channel from a membrane fraction enriched in contractile vacuole of Dictyostelium discoideum. *Biochim. Biophys. Acta* **1325**, 178-188.

Zeuthen, T. (1992). From contractile vacuole to leaky epithelia. Coupling between salt and water fluxes in biological membranes. *Biochim. Biophys. Acta* **1113**, 229-258.

Additional Information

Contributions

FX, XW, L-HJ, HZ and JP designed the experiments and analyzed the data. FX and XW conducted the experiments. FX, L-HJ, HZ and JP wrote the paper.

Competing financial interests

The authors declare no competing financial interests.

Figure Legends

Fig. 1. Analysis of K^+ channels in *C. reinhadtii*

(A) Sequence alignments of 14 identified K+ channels of *C. reinhardtii* together with K^+ channels from human (KCNH1, O95259) and *Arabidopsis* (SKOR, Q9M8S6). Only the K^+ filter selection regions and the voltage sensor segments are presented. The consensus amino acids are shown below the alignments. Except for IRK1, all the *C. reinhardtii* K^+ channels possess the positively charged voltage sensor domain.

(B) Phylogenetic analysis. The transmembrane regions of 14 putative K^+ channels were analyzed together with those of representative members from subgroups of K^+ channels in human and *Arabidopsis*. Branch length indicates evolutionary distance. Please see Materials and Methods for detail. Black, members from *Chlamydomonas*; green, members from higher plants; blue, members from human.

Fig. 2. A *C. reinhardtii* insertional mutant is defective in *KCN11*, which encodes an outwardly rectifying K^+ channel

(A) Schematic diagram of the *KCN11*gene structure showing the foreign DNA insertion site in the sixth axon. Grey marks the foreign DNA fragment containing the *AphVIII* gene with part sequence being shown. Brown shows the flanking sequence of the insert. The insertion site was identified by PCR and DNA sequencing.

(B) Domain structure and topology of KCN11. S1-S6, transmembrane segments; P, pore loop; S, K^+ selective signature motif; cNMP, cNMP binding domain; and LCR, low complexity regions.

(C) *kcn11* mutant exhibits no KCN11 expression analyzed by quantitative RT-PCR. The expression of *Chlamydomonas* Beta Subunit-like Polypeptide (CBLP) was used for normalization. Data shown are mean and SEM from three independent experiments.

(D) Representative current recordings from untransfected HEK cells or cells transfected with *KCN11* or with a K^+ selective filter mutant (T392G/V394E/G395E). For blocker experiments, the extracelluar solution contained 1 mM

Tetraethylammonium chloride (TEA), 10 μM nifedipine, or 1 μM Tetrodotoxin (TTX). Cells were held at -60 mV. Step protocols (-100 to +60 mV with 10 mV increment) were applied.

(E) I-V curves of peak K^+ current densities in untransfected cells (n=6), *KCN11* transfected cells in the absence (n=8) or presence of TEA (n=7), nifedipine (n=7), TTX (n=6) and *KCN11* filter mutant transfected cells (n=7). Same recording protocols are as in (D). Data shown are mean and SEM.

(F) I-V curves of the peak K^+ current densities in *KCN11* transfected cells in the extracellular solutions containing different K+ concentrations (mM) as indicated and 140 mM intracellular solutions (n=6-8). Data shown are mean and SEM.

(G) The current reversal potentials derived from the I-V curves shown in (F) were plotted against the extracellular potassium concentrations. Line is fitted to $E_{rev} = 62\log([K]_o / 140)$.

Fig. 3. KCN11 is localized to the CV membrane

(A) WT and *kcn11*::*KCN11*-HA cells were immunostained with anti-HA and anti-α-tubulin antibodies, respectively. Insets are enlarged images. Bar, 5 μm.

(B) Three-dimensional reconstruction of immunostained cell images. Please note, KCN11 staining is localized in two irregular bladder-like structures. Bars, 2 μm.

Fig. 4. KCN11 is required for CV contraction and osmoregulation

(A) Still images from Movie S1-S4 showing the CV contraction of WT and *kcn11* cells in growing medium or water. Arrow heads mark the recorded CV. Bar, 5 μm.

(B) Statistical analysis of the CV periods. Data shown are mean and SEM (n=45 cells). Asterisks indicate statistically significant differences (*t* test, $p<0.0001$). N.S., no significant.

(C) CV diameters of WT and *kcn11* cells in growing medium or water. Data shown are from 30 cells from each analysis.

(D) Cell growth for three days on agar plates prepared with distilled water.

(E) Representative images of water-grown cells stained with FDA. Yellow cells,

FDA-stained live cells. Red cells, dead cells showing autofluorescence of chlorophyll. Bar, 5 μm.

(F) Cell viability grown in water. Cells were grown in water for three days. Cell viability was scored by fluorescein diacetate (FDA) staining. At least 300 cells were scored from each time point. Data shown are mean and SEM from three independent experiments.

Fig.1 Xu et al.,

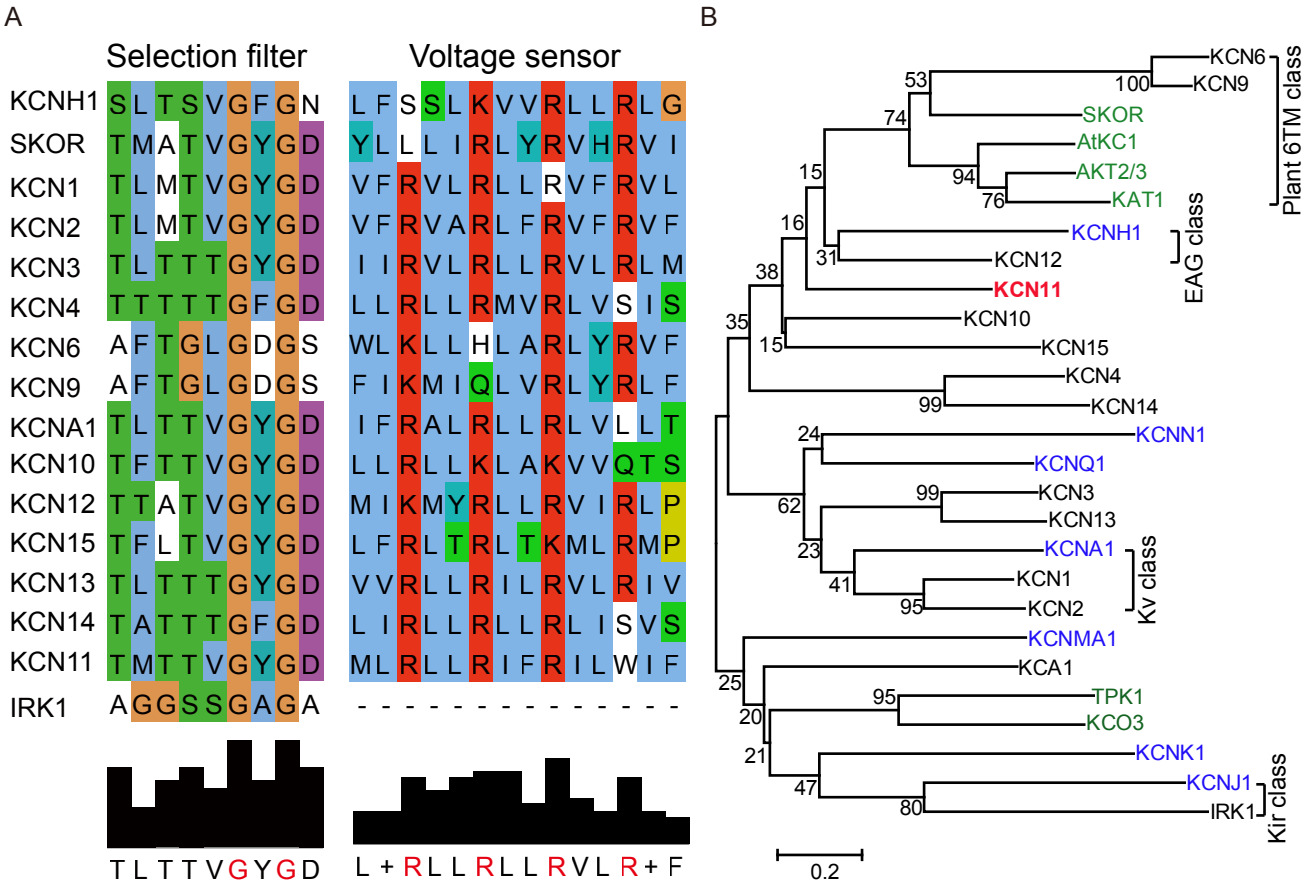
A
Selection filter
Voltage sensor
KCNH1 S L T S V G F G N L F S S L K V V R L L R L G
SKOR T M A T V G Y G D Y L L L I R L Y R V H R V I
KCN1 T L M T V G Y G D V F R V L R L L R V F R V L
KCN2 T L M T V G Y G D V F R V A R L F R V F R V F
KCN3 T L T T T G Y G D I I R V L R L L R V L R L M
KCN4 T T T T T G F G D L L R L L R M V R L V S I S
KCN6 A F T G L G D G S W L K L L H L A R L Y R V F
KCN9 A F T G L G D G S F I K M I Q L V R L Y R L F
KCNA1 T L T T V G Y G D I F R A L R L L R L V L L T
KCN10 T F T T V G Y G D L L R L L K L A K V V Q T S
KCN12 T T A T V G Y G D M I K M Y R L L R V I R L P
KCN15 T F L T V G Y G D L F R L T R L T K M L R M P
KCN13 T L T T T G Y G D V V R L L R I L R V L R I V
KCN14 T A T T T G F G D L I R L L R L L R L I S V S
KCN11 T M T T V G Y G D M L R L L R I F R I L W I F
IRK1 A G G S S G A G A - - - - - - - - - - - - - -
T L T T V G Y G D
L + R L L R L L R V L R + F
B
KCN6
KCN9
SKOR
AtKC1
AKT2/3
KAT1
KCNH1
KCN12
KCN11
KCN10
KCN15
KCN4
KCN14
KCNN1
KCNQ1
KCN3
KCN13
KCNA1
KCN1
KCN2
KCNMA1
KCA1
TPK1
KCO3
KCNK1
KCNJ1
IRK1
53
100
74
94
76
15
16
31
38
35
15
99
24
99
62
23
41
95
25
95
20
21
47
80
Plant 6TM class
EAG class
Kv class
Kir class
0.2

Fig.2 Xu et al.,

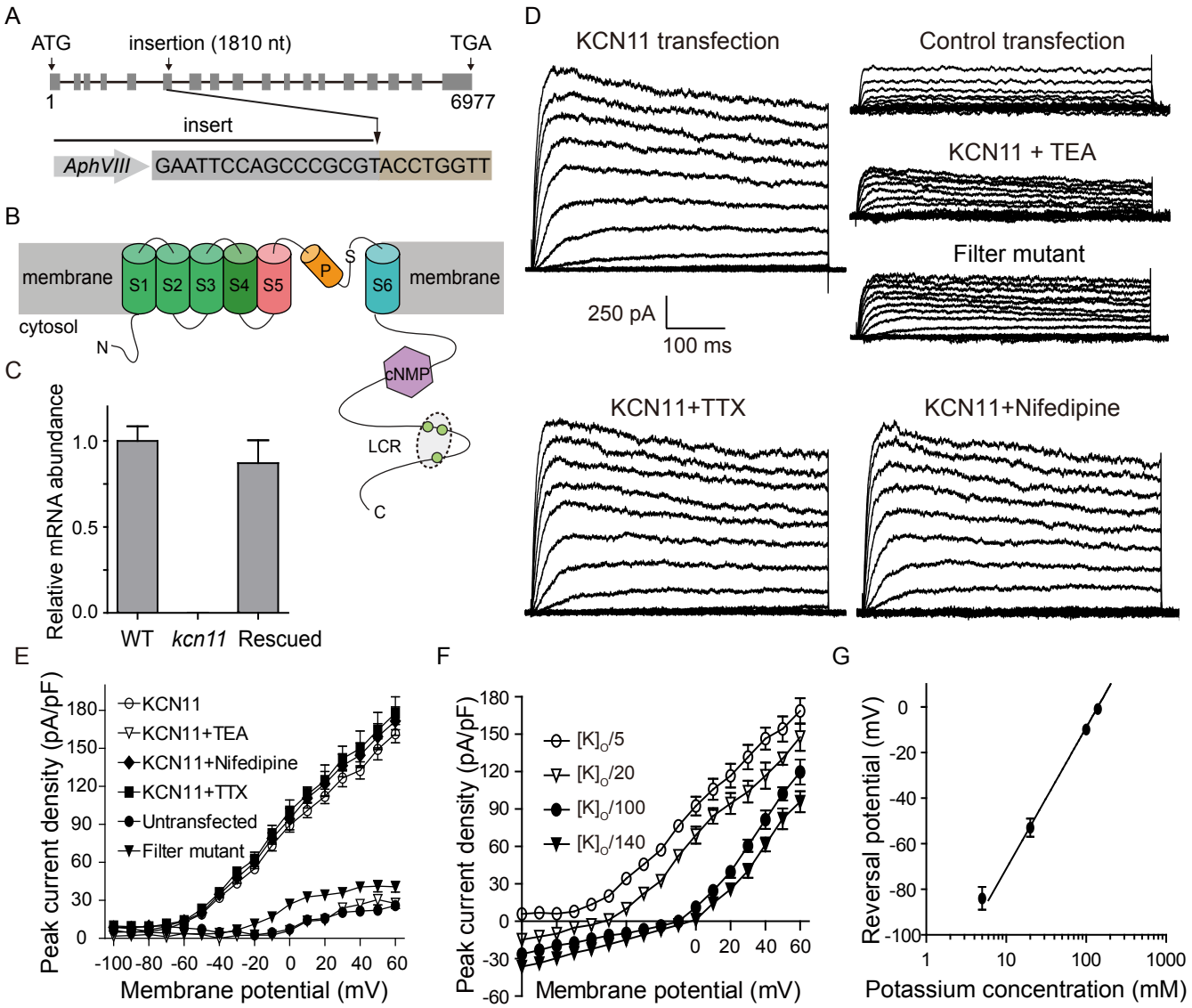
A
ATG
insertion (1810 nt)
TGA
1
6977
insert
AphVIII
GAATTCCAGCCCGCGTACCTGGTT
B
membrane
S1
S2
S3
S4
S5
P
S
S6
membrane
cytosol
N
cNMP
LCR
C
C
Relative mRNA abundance
1.0
0.5
0.0
WT
kcn11
Rescued
D
KCN11 transfection
Control transfection
KCN11 + TEA
Filter mutant
250 pA
100 ms
KCN11+TTX
KCN11+Nifedipine
E
Peak current density (pA/pF)
KCN11
KCN11+TEA
KCN11+Nifedipine
KCN11+TTX
Untransfected
Filter mutant
Membrane potential (mV)
F
Peak current density (pA/pF)
[K]o/5
[K]o/20
[K]o/100
[K]o/140
Membrane potential (mV)
G
Reversal potential (mV)
Potassium concentration (mM)

Fig.3 Xu et al.,

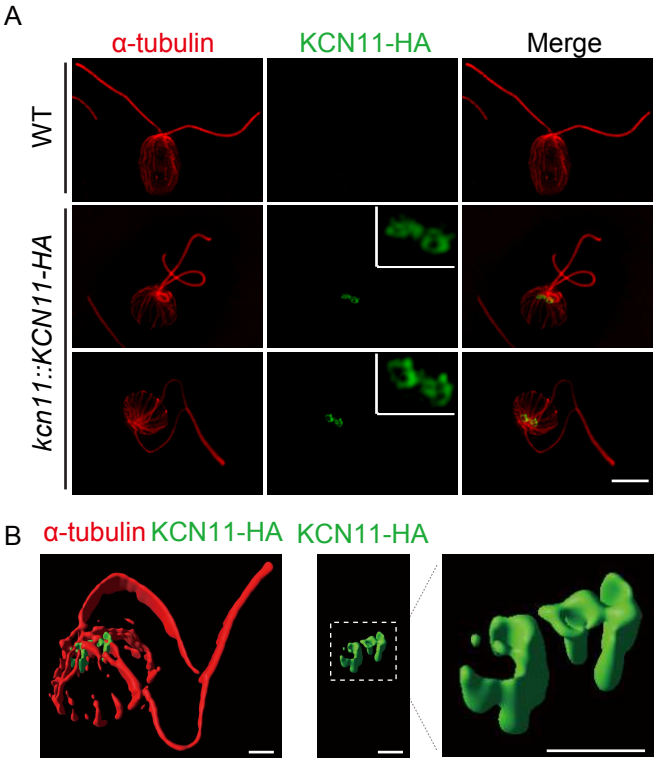
A
α-tubulin
KCN11-HA
Merge
WT
kcn11::KCN11-HA
B
α-tubulin KCN11-HA
KCN11-HA

Fig.4 Xu et al.,

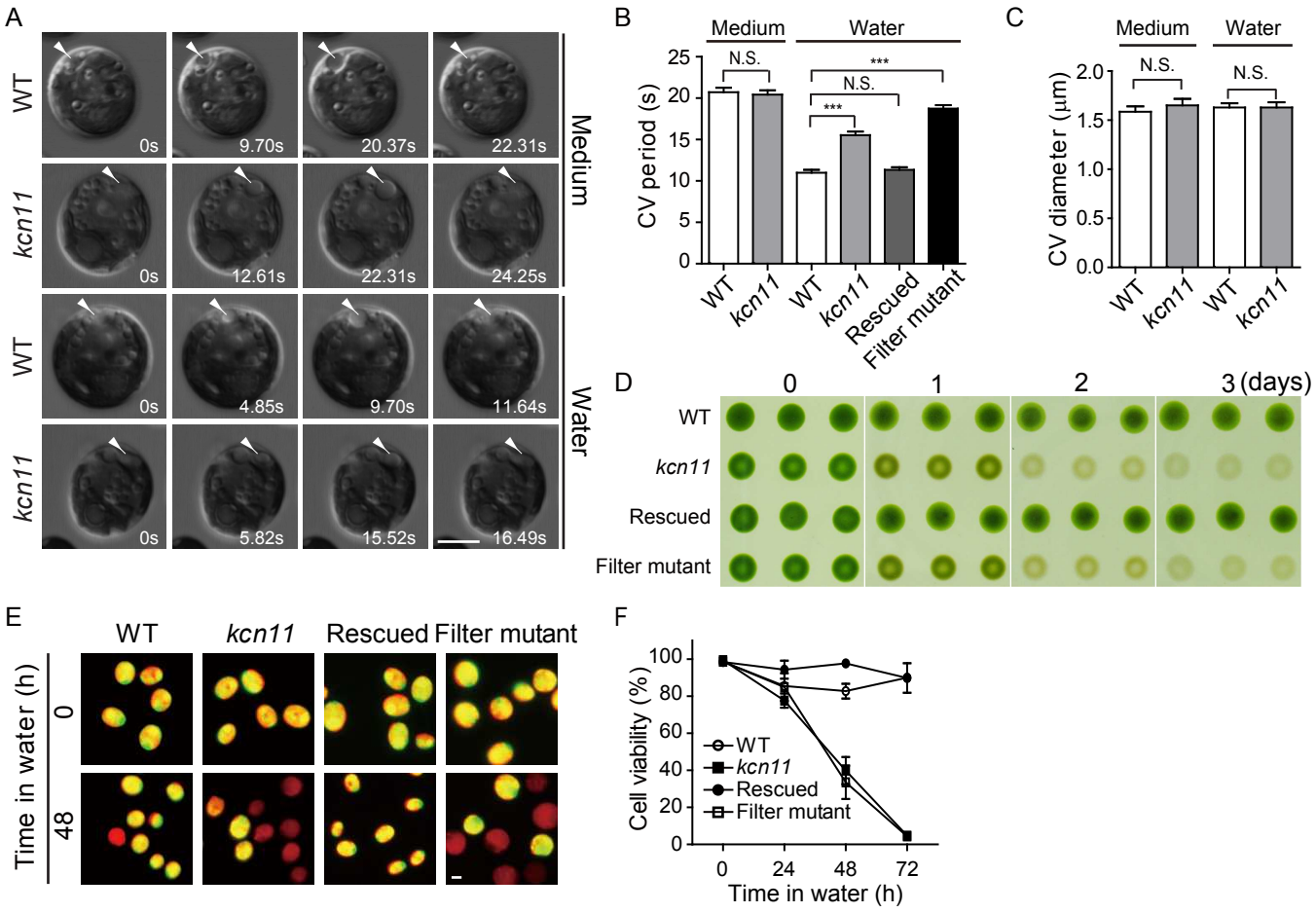
A
WT
kcn11
WT
kcn11
0s
9.70s
20.37s
22.31s
0s
12.61s
22.31s
24.25s
0s
4.85s
9.70s
11.64s
0s
5.82s
15.52s
16.49s
Medium
Water
B
Medium
Water
CV period (s)
N.S.
N.S.
***
***
WT
kcn11
WT
kcn11
Rescued
Filter mutant
C
Medium
Water
CV diameter (μm)
N.S.
N.S.
WT
kcn11
WT
kcn11
D
0
1
2
3 (days)
WT
kcn11
Rescued
Filter mutant
E
WT
kcn11
Rescued
Filter mutant
Time in water (h)
0
48
F
Cell viability (%)
WT
kcn11
Rescued
Filter mutant
Time in water (h)